Evaluation of Confining Pressure Models for Circular Concrete-Filled Steel Tube Short Columns under Concentric Loading

Hoang An Le
Ho Chi Minh City University of Transport, Vietnam
hoangan.le@ut.edu.vn
(corresponding author)

Received: 5 December 2022 | Revised: 2 January 2023 | Accepted: 5 January 2023

ABSTRACT

It is well known that the confinement effect provided by the steel tube significantly increases the strength and ductility of circular Concrete Filled Steel Tube (CFST) columns under concentric loading. The lateral pressure is an important factor to calculate the strength enhancement of CFST columns. To reliably predict the ultimate strength of circular CFST columns, many models have been developed for predicting the lateral pressure due to the confinement effect. This paper aims to evaluate some of these confining pressure models. The values of the compressive strength of confined concrete and lateral confining pressure of circular CFST short columns were calculated using these existing models and were compared with those obtained from previous test results. In addition, a comparison between the ultimate loads predicted by these models and by Eurocode 4 (EC4) was carried out. Based on the comparison results, some suitable models for circular CFST short columns with the use of normal-strength, high-strength, and ultra-high-strength concrete were indicated.

Keywords-concrete filled steel tube columns; confinement effect; strength enhancement; steel tube; confining pressure

I. INTRODUCTION

The composite action between the steel tubes and the concrete core leads to the strength enhancement of Concrete Filled Steel Tube (CFST) columns [1, 19]. The steel tube provides confining pressure to the concrete core and shares the axial load, which puts the concrete core under a triaxial state of stress while the steel tube is stressed biaxially [1-3]. In addition, the steel tube is more stiffened by the concrete core. The inward buckling of the steel tube is prevented by the concrete core, thus leading to an increase in the stability as well as the strength of the column [4]. Circular CFST columns exhibit better gain of load capacity due to the effectiveness of the confinement effect as compared with square or rectangular CFST columns [1]. Therefore, the circular CFST columns are recommended to be used in practice to obtain better strength and ductility [19-21]. To calculate the ultimate strength of circular CFST columns, the lateral pressure induced by the steel tube on the concrete core should be accurately estimated. Because the measurement of lateral pressure in the real test is very complicated, many researchers have proposed models to predict the lateral pressure. Authors in [3] tried to find the stress-strain relationship and the ultimate strength of concrete inside CFST columns with considering the Poisson's ratios. The lateral confining pressure of the steel tube on the concrete was calculated at the point that the steel is in the plastic range and the concrete core is completely crushed. Authors in [15] proposed a confining pressure model for concrete in CFST columns by taking into account the effect of geometry and material properties on the strength enhancement and post-peak behavior. Authors in [3] modified the models in [4, 5] for CFST columns. Authors in [6] developed a uniaxial stress-strain relationship for concrete confined by various shaped steel tubes. In [1], the efficiency of the steel tube in confining the concrete core was examined by investigating the effects of concrete strength and steel tube thickness. Authors in [7] also developed a confining pressure model for concrete in circular, square, and octagonal CFST columns by employing the nonlinear finite element method in ABAQUS. Authors in [8] suggested a model to calculate the ultimate strength of the concrete core in CFST columns depending on the hoop stress of steel tube at yield condition. Authors in [9] proposed models for predict the ultimate load of circular CFST under extreme loading conditions with the use a new empirical equation for estimate the hoop stress of the steel tube. Authors in [10] proposed an accurate model for confined concrete and a new design formula for determining the ultimate axial loads of CFST columns using Normal Strength Concrete (NSC) and High Strength Concrete (HSC). Authors in [11] presented a full elasto-plastic model and a simplified model for CFST stub columns with concrete strength ranging from 30 to 120MPa and diameter-to-wall thickness (D/t) greater than 20. All collected models have been mainly developed for NSC and

HSC filled in steel tubes. Nevertheless, the application of these models for Ultra-High Strength Concrete (UHSC) is still questionable. Therefore, there is a need to investigate the suitability of these models for circular CFST short columns with various concrete strengths, i.e. NSC, HSC, and UHSC.

Based on the aforementioned issues, this paper aims to evaluate the existing models [1, 2, 6, 8-11] through the comparison between the predictions and the test results. The ultimate loads and lateral confining pressures of circular CFST columns under the concentric compression on the entire section from some previous experimental tests were calculated using the equations of the existing models. Furthermore, the prediction of ultimate loads from Eurocode 4 (EC4) was also compared with the predictions obtained from the existing models. The findings of this paper indicate suitable models for the estimation of the ultimate load and confining pressure of circular CFST short columns.

II. CONFINING PRESSURE MODELS AND TEST DATABASE

The considered confining pressure models for circular CFST short columns [1, 2, 6, 8-11] were collected and are shown in Table I. These models were used for the prediction of confining pressure and ultimate load of the previous tests.

TABLE I. EXPRESSIONS OF CONFINING PRESSURE MODELS FOR CIRCULAR CFST SHORT COLUMNS

Model	Expression	Explanation
[6]	$\nu_c' = \frac{0.881}{10^6}.\left(\frac{D}{t}\right)^3 - \frac{2.58}{10^4}.\left(\frac{D}{t}\right)^2 + \frac{1.953}{10^2}.\left(\frac{D}{t}\right) + 0.4011$ $\nu_c = 0.2312 + 0.3528.\nu_c' - 0.1524.\left(\frac{f_c}{f_y}\right) + 4.843.\nu_c'.\left(\frac{f_c}{f_y}\right) - 9.169.\left(\frac{f_c}{f_y}\right)^2 ; \beta = \nu_c - \nu_s;$ $f_{rp} = \beta\frac{2t}{D-2t}f_y ; f_{cc} = f_c + 4.f_{rp}; N_u = A_c.f_{cc} + A_a.f_y$	ν_c': Empirical factor. ν_s: Poisson ratio of a steel tube, taken equal to 0.5. f_{rp}: Lateral pressure at the peak load. f_{cc}: Confined compressive strength of concrete. N_u: Axial capacity of CFST column.
[9]	$\sigma_h = f_y.\exp\left[\ln\left(\frac{D}{t}\right) + \ln(f_y) - 11\right].f_y ; f_{rp} = \frac{2t}{D-2t}\sigma_h; f_{cc}' = f_c' + k_1.f_{rp}$ $f_y = 0.5.\left(\sigma_h - \sqrt{4.f_y^2 - 3.\sigma_h^2}\right); N_u = A_c.f_{cc} + A_a.f_y$	σ_h: Hoop stress of the steel. f_y: Yield strength of steel.
[1]	$\nu_a = 0.3, \nu_c = 0.2, \varepsilon_v = 0.002 ; \varepsilon_{ahr} = \frac{\varepsilon_v.(\nu_a - \nu_c)}{\left[1 + \frac{2.t.E_a}{(D-2.t).E_c}\right]}$ $\varepsilon_{ah} = -\nu_a.\varepsilon_v + \varepsilon_{ahr} ; \sigma_h = \frac{E_a}{1-\nu_a^2}.(\varepsilon_{ah} + \nu_a.\varepsilon_{al});$ $\sigma_{al} = \frac{E_a}{1-\nu_a^2}.(\varepsilon_v + \nu_a.\varepsilon_{ah}) ; \sigma_{lat} = \sigma_{ah}.\frac{2.t}{D-2.t}; k = 1.25.\left(1 + 0.062.\frac{\sigma_{lat}}{f_{ct}}\right).f_c^{-0.21}.f_c$ $f_{cc} = f_c.\left(\frac{\sigma_{lat}}{f_{ct}} + 1\right)^k ; N_u = A_c.f_{cc} + A_a.\sigma_{al}$	$\nu_a, \nu_c, \varepsilon_v$: Initial considered values. ε_{ahr}: Restrained steel strain. ε_{ah}: Final lateral strain of steel. σ_{al}: Steel's longitudinal stress. σ_{lat}: Compressive confining pressure. k: Reflects the effectiveness of confinement. f_{ct}: Tensile strength of concrete.
[11]	$f_{cc} = f_c + 3.4.\sigma_{r,c} ; \frac{\sigma_{r,c}}{f_c} = \frac{\emptyset(k-1)}{\sqrt{9+3(k-1)^2}} ; F_{Fa} = f_c.A_c(1 + \frac{k\emptyset}{2})$	$\sigma_{r,c}$: Confining pressure around the concrete. $\emptyset$: confinement index, $=\frac{f_s.A_s}{f_c.A_c}$ k=3 ÷ 4.3
[8]	$\sigma_{ccB} = \gamma_U.f_c' + 4.1.\sigma_r ; \gamma_U = 1.67D_c^{-0.112} ; \sigma_r = \frac{-2t}{D-2t}\sigma_{s\theta}$ $\sigma_{s\theta} = \alpha_u.\sigma_{sy}$ with $\alpha_u = -0.19$ $\sigma_{sz} = \beta_{uc}.\sigma_{sy}$ with $\beta_{uc} = 0.89$ $N_u = (A_c.\sigma_{ccB} + A_s.\sigma_{sz})$	σ_{ccB}: Strength of confined concrete. γ_u: Strength reduction factor for concrete. σ_r: Lateral pressure. $\sigma_{s\theta}$: Hoop stress of steel tube in yield condition. σ_{sy}: Tensile yield stress of steel tube. σ_{sz}: Axial yield stress of steel tube.
[10]	$f_{cc}' = \gamma_c.f_c' + k_1.f_{rp}$ $f_{rp} = \begin{cases} 0.7(\nu_e - \nu_s)\frac{2t}{D-2t}f_{sy} & \text{for } \frac{D}{t} \le 47 \\ \left(0.006241 - 0.0000357\frac{D}{t}\right)f_{sy} & \text{for } 47 \le \frac{D}{t} \le 150 \end{cases}$ $\nu_e = 0.2312 + 0.3528.\nu_e' - 0.1524.\frac{f_c'}{f_{sy}} + 4.843.\nu_c'.\frac{f_c'}{f_{sy}} - 9.169.\left(\frac{f_c'}{f_{sy}}\right)^2$ $\nu_e' = \frac{0.881}{10^6}.\left(\frac{D}{t}\right)^3 - \frac{2.58}{10^4}.\left(\frac{D}{t}\right)^2 + \frac{1.953}{10^2}.\left(\frac{D}{t}\right) + 0.4011$ $\gamma_c = 1.85D_c^{-0.135}$ for $(0.85 \le \gamma_c \le 1.0) ; \gamma_s = 1.458\left(\frac{D}{t}\right)^{-0.1}$ for $(0.9 \le \gamma_s \le 1.1)$ $N_u = \left(\gamma_c f_c' + 4.1.f_{rp}\right)A_c + \gamma_s f_{sy}A_s$	f_{cc}': Strength of confined concrete. f_{rp}: Lateral pressure. γ_c: Strength reduction factor for concrete. γ_s: Strength factor for steel tube. f_{sy}: Tensile yield strength of steel. ν_e': Empirical factor. ν_e : Poisson ratio of a steel tube filled with concrete
[3]	$p_0 = -\frac{\alpha}{2}\frac{2\mu'+1}{[3(\mu'^2+\mu'+1]^{\frac{1}{2}}}f_y ; \mu' = -\frac{1}{2} - \frac{1}{2(\xi+1)} ; \xi = \alpha\frac{f_y}{f_c}$ $\alpha = \frac{A_s}{A_c} ; N_u = N_c + N_s ; N_s = \frac{\mu'+2}{[3(\mu'^2+\mu'+1]^{\frac{1}{2}}}f_yA_s$ $N_c = (f_c + 4p_0)A_c$	p_0: Lateral confining pressure of the steel tube on concrete. N_c: Sectional strength of concrete core. N_s: Sectional strength of steel tube.

A total of 178 circular CFST columns were chosen for the calculation. These columns were tested under concentric compression on the entire section. Dimensions and material properties of the selected columns are summarized in Tables II and III. The main dimensions of the columns are described by the outer diameter (D), the thickness of steel tube (t), and the length of the columns (L). The material properties include the unconfined concrete strength (f_c) and the yield strength of the steel tube (f_y). The selected columns were divided into 2 groups: (1) group 1 includes CFST short columns with NSC ($f_c \le 60$MPa), (2) group 2 includes CFST short columns with HSC (60MPa < $f_c \le 120$MPa) and UHSC ($f_c > 120$MPa). The test database covers a wide range of concrete strengths.

TABLE II. TEST DATABASE OF CIRCULAR CFST COLUMNS USING NSC (GROUP 1)

Tested by	D (mm)	t (mm)	L (mm)	fc (MPa)	fy (MPa)
[13], 18 specimens	76.4-152.6	1.68-4.09	152.3-304.9	20.9-40.9	363.3-451.6
[14], 26 specimens	101.0-318.5	3.03-10.37	305-955	23.2-52.2	371-452
[15], 42 specimens	76.5-300	1.5-4.5	276-1000	20.54-45.77	232.3-433.2

TABLE III. TEST DATABASE OF CIRCULAR CFST COLUMNS USING HSC AND UHSC (GROUP 2)

Tested by	D (mm)	t (mm)	L (mm)	fc (MPa)	fy (MPa)
[15], 18 specimens	108-133	1.0-7.0	378-465	106-116	232-429
[16], 26 specimens	60-250	1.87-2.0	180-750	85.2-90.0	282-404
[17], 21 specimens	101.6-139.8	2.37-3.0	304.8-419.4	62.4-135.6	341-462.6
[18], 27 specimens	149-165	1.0-6.0	500	87.1-91.8	338-438

The models proposed in [1, 2, 6, 8-11] were used to predict the axial capacity and lateral confining pressure of circular CFST columns. However, the model of [6] is only applicable for f_c/f_y ranging from 0.04 to 0.2. The columns with HSC and UHSC have $f_c/f_y > 0.2$, thus the model of [6] was not further considered.

For the assessment of the accuracy of the prediction, two statistical indicators were determined, the Mean Square Error (MSE) and the Average Absolute Error (AAE):

$$MSE = \frac{\sum_1^n \left(\frac{pre_i - exp_i}{exp_i}\right)^2}{N} \quad (1)$$

$$AAE = \frac{\sum_1^n \left|\frac{pre_i - exp_i}{exp_i}\right|}{N} \quad (2)$$

where pre_i represents values of ultimate load from model predictions, exp_i represents the values of ultimate load from the experimental results, and N is the total number of test data.

The confinement ratio Ø is defined by:

$$\emptyset = \frac{A_s.f_y}{A_c.f_c} \quad (3)$$

where A_s is the area of steel section, while A_c is the area of concrete section.

III. RESULTS AND DISCUSSION

The relation between the ratios f_{cc}/f_c and f_l/f_c, where f_l is the lateral confining pressure and f_{cc} is the confined concrete strength, is shown in Figure 1. It can be seen that all the models describe a quite similar trend. This relation can be represented by a linear equation. As the ratio f_l/f_c increases, the ratio f_{cc}/f_c also increases considerably in the case of group 1 while the increment of f_{cc}/f_c is slighter in the case of group 2, due to the higher confinement when employing NSC for CFST columns. It could be observed that in group 1, the models of [6, 8, 9] exhibit the same predicting value of f_{cc}/f_c at a given value of f_l/f_c, whereas the scatter plots of the other models show a different tendency. Furthermore, in group 2, the models suggested by [2, 8-11] are rather close to each other, while the model of [1] gives an unlikely trend. Figure 2 illustrates the predicted value of confining pressure f_l versus the confinement ratio Ø.

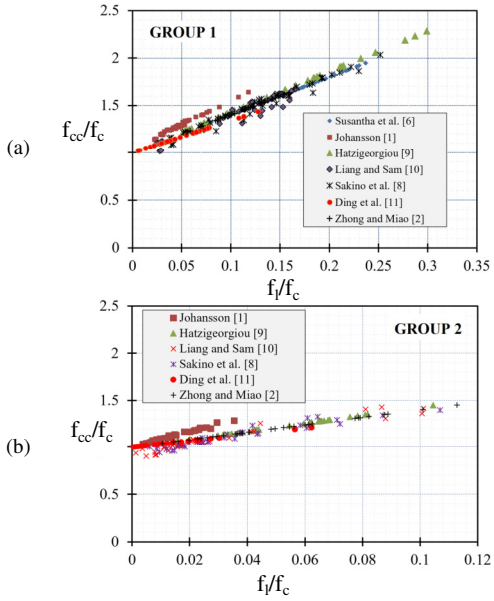

Fig. 1. Comparison of models in prediction of f_{cc}/f_c and f_l/f_c.

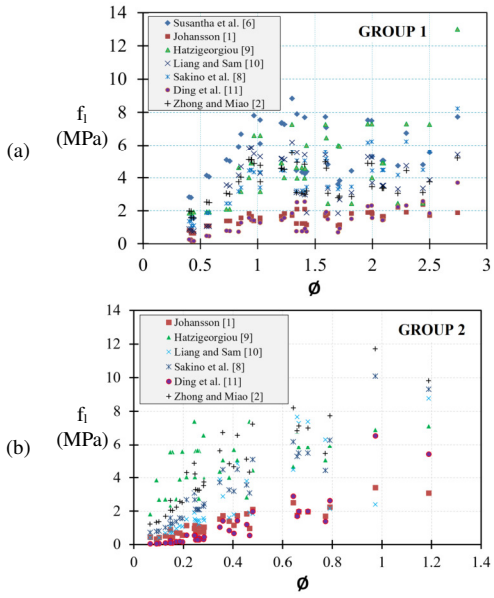

Fig. 2. Comparison of models in prediction of confining pressure f_l.

Overall, the graph indicates the variation of confining pressure f_l corresponding to each model. It can be seen that when the confinement ratio increases, the confinement pressure shows an upward trend. The models of [1, 11] exhibited a very low value of confining pressure in comparison with the other models, while the models of [6, 9] presented the highest values. It is evident from the data that the confining pressure predicted from [10] was very close to [2] in the case of group 1. Moreover, the model of [2] gives higher values of f_l in the case

of group 2. It is apparent from the scatter plot that the confinement ratio Ø has no correlation with the confining pressure. The above results can be explained by the fact that except for the model of [10], all models consider high confining pressure of steel tube in circular CFST stub columns. However, the confining pressure of steel tube decreases with increasing concrete strength.

Figure 3 shows the comparison of ultimate load between model predictions (N_{pre}) and EC4 [12] predictions (N_{EC4}). In order to better reflect the deviations of prediction as compared to experimental results and EC4 [12], the -10% and +10% error bounds depicted in the Figure are presented in the following sub-sections. It has been demonstrated in group 1 that the predictions from [8-10] are quite close to those from EC4 [12] (around 10%), while the models from [2, 11] give less accurate values (about 20% higher and 20% lower on average, respectively). At the same time, the predictions by [1, 6] have varying values. Interestingly, it could be observed in group 2 that almost all models except the one of [11] have very close values (within 10%) to the ones of [12]. The agreement of EC4 and the predicted models is generally good. It should be noted that EC4 is applicable with concrete strength up to 70MPa. Therefore, the prediction by EC4 is less accurate for the circular CFST columns having concrete strength higher than 70MPa.

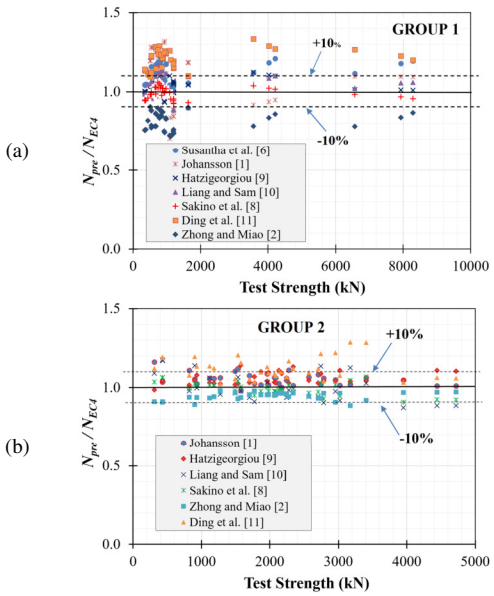

Fig. 3. Comparison of ultimate loads between the model predictions and EC4 [12].

The comparison between the ultimate strength from the real tests (N_{test}) and the calculated strength from the models (N_{pre}) is illustrated in Figure 4. Regarding group 1, the predictions of [6, 9, 10] give a quite good correlation with the test data (around 10%), whereas the models from [2, 11] exhibit large differences between the experimental and the predicted values. In addition, all models except the ones from [6, 11] generally tend to underestimate the strength of CFST columns when the test strength increases. Figure 4 clearly indicates that almost all models show a large variability in individual prediction. However, the models from [8, 10] give a better precision than the other models in estimating the ultimate strength. On the other hand, the models from [1, 9, 11] overestimate these values. The models from [8, 10] use the strength reduction factor for concrete depending on the outer diameter of the concrete core. Therefore, these models give ultimate load prediction smaller than the other models.

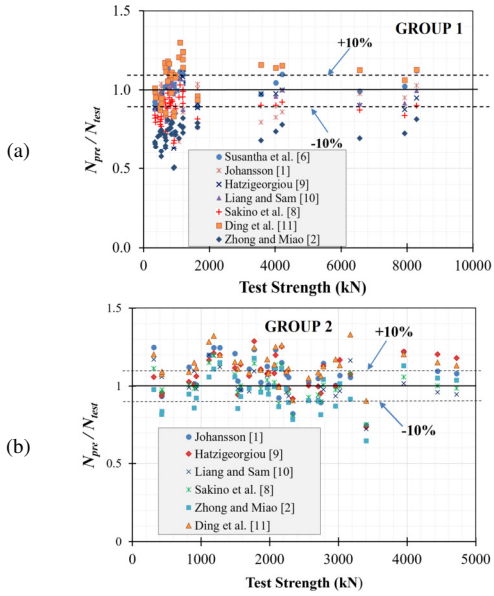

Fig. 4. Comparison of ultimate loads between the model predictions and the test results.

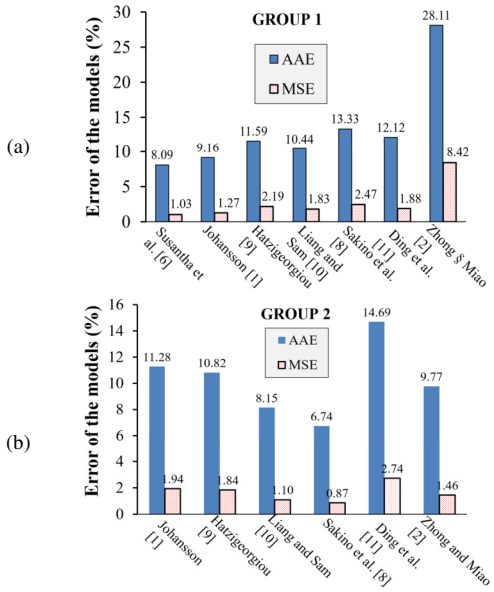

Fig. 5. Comparison of statistical indicators AAE and MSE.

Based on the two statistical indicators, AAE and MSE, shown in Figure 5 for the CFST stub columns employing NSC, the models from [1, 6] provide the best prediction of ultimate

strength because they have the smallest error (just under 9%), followed by the model from [10] with error around 10%. The models proposed in [8, 9, 11] show a good prediction, with error greater than 10%. Conversely, the error of the model from [2] is larger, thus this model should not be used for estimating the ultimate strength of NSC filled in steel tube stub columns.

Regarding group 2, Figure 5 shows that the models from [8, 10] give the smallest error. The errors in the prediction of ultimate strength in CFST columns using HSC and UHSC are much larger than those in CFST columns using NSC. This may partly be caused by the less effective confinement of CFST columns using higher strength concrete core, while almost all existing models consider the passive confinement in calculating the confined strength of concrete core.

IV. CONCLUSION

In this paper, models for predicting the lateral confining pressure of circular CFST short columns were considered and used for the calculation of the lateral stress and ultimate load of the tested columns. The main conclusions derived from the findings of this paper are:

- Almost all models give more accurate predictions for circular CFST short columns using NSC than HSC and UHSC.
- The prediction is less accurate with increasing concrete strength.
- There are significant differences among the models in lateral stress prediction.
- The models suggested in [8, 10] are suitable for predicting the ultimate strength of CFST columns with HSC and UHSC.
- The models of [1, 6] give accurate prediction of the ultimate strength for CFST columns using NSC.
- The ultimate load prediction obtained by the model of [11] is close to the ultimate load predicted by EC4 [12].

REFERENCES

[1] M. Johansson, "The efficiency of passive confinement in CFT columns," *Steel and Composite Structures*, vol. 2, no. 5, pp. 379–396, Oct. 2002, https://doi.org/10.12989/scs.2002.2.5.379.

[2] Z. Shan-Tong and M. Ruo-Yu, "Stress-Strain Relationship and Strength of Concrete Filled Tubes," presented at the Composite Construction in Steel and Concrete, Henniker, NH, USA, 1988, pp. 773–785.

[3] M. D. O'Shea and R. Q. Bridge, "Design of Circular Thin-Walled Concrete Filled Steel Tubes," *Journal of Structural Engineering*, vol. 126, no. 11, pp. 1295–1303, Nov. 2000, https://doi.org/10.1061/(ASCE)0733-9445(2000)126:11(1295).

[4] J. B. Mander, M. J. N. Priestley, and R. Park, "Theoretical Stress-Strain Model for Confined Concrete," *Journal of Structural Engineering*, vol. 114, no. 8, pp. 1804–1826, Aug. 1988, https://doi.org/10.1061/(ASCE)0733-9445(1988)114:8(1804).

[5] M. M. Attard and S. Setunge, "Stress-Strain Relationship of Confined and Unconfined Concrete," *Materials Journal*, vol. 93, no. 5, pp. 432–442, Sep. 1996, https://doi.org/10.14359/9847.

[6] K. A. S. Susantha, H. Ge, and T. Usami, "Uniaxial stress–strain relationship of concrete confined by various shaped steel tubes," *Engineering Structures*, vol. 23, no. 10, pp. 1331–1347, Oct. 2001, https://doi.org/10.1016/S0141-0296(01)00020-7.

[7] H.-T. Hu, C.-S. Huang, M.-H. Wu, and Y.-M. Wu, "Nonlinear Analysis of Axially Loaded Concrete-Filled Tube Columns with Confinement Effect," *Journal of Structural Engineering*, vol. 129, no. 10, pp. 1322–1329, Oct. 2003, https://doi.org/10.1061/(ASCE)0733-9445(2003)129:10(1322).

[8] H.-T. Hu, C.-S. Huang, M.-H. Wu, and Y.-M. Wu, "Nonlinear Analysis of Axially Loaded Concrete-Filled Tube Columns with Confinement Effect," *Journal of Structural Engineering*, vol. 129, no. 10, pp. 1322–1329, Oct. 2003, https://doi.org/10.1061/(ASCE)0733-9445(2003)129:10(1322).

[9] G. D. Hatzigeorgiou, "Numerical model for the behavior and capacity of circular CFT columns, Part I: Theory," *Engineering Structures*, vol. 30, no. 6, pp. 1573–1578, Jun. 2008, https://doi.org/10.1016/j.engstruct.2007.11.001.

[10] Q. Q. Liang and S. Fragomeni, "Nonlinear analysis of circular concrete-filled steel tubular short columns under axial loading," *Journal of Constructional Steel Research*, vol. 65, no. 12, pp. 2186–2196, Dec. 2009, https://doi.org/10.1016/j.jcsr.2009.06.015.

[11] F. Ding, Z. Yu, Y. Bai, and Y. Gong, "Elasto-plastic analysis of circular concrete-filled steel tube stub columns," *Journal of Constructional Steel Research*, vol. 67, no. 10, pp. 1567–1577, Oct. 2011, https://doi.org/10.1016/j.jcsr.2011.04.001.

[12] *Eurocode 4, Design of Composite Steel and Concrete Structures, Part 1.1, General Rules and Rules for Buildings*. Brussels, Belgium: CEN, 2004.

[13] N. J. Gardner and E. R. Jacobson, "Structural Behavior of Concrete Filled Steel Tubes," *Journal Proceedings*, vol. 64, no. 7, pp. 404–413, Jul. 1967, https://doi.org/10.14359/7575.

[14] T. Yamamoto, J. Kawaguchi, and S. Morino, "Experimental Study of Scale Effects on the Compressive Behavior of Short Concrete-Filled Steel Tube Columns," in *Composite Construction in Steel and Concrete IV Conference 2000*, Apr. 2012, pp. 879–890, https://doi.org/10.1061/40616(281)76.

[15] J. Tang, S. Hino, I. Kuroda, and T. Ohta, "Modeling of Stress - Strain Relationships for Steel and Concrete in Concrete Filled Circular Steel Tubular Columns," *Steel Construction Engineering*, vol. 3, no. 11, pp. 35–46, 1996, https://doi.org/10.11273/jssc1994.3.11_35.

[16] L.-H. Han, W. Li, and R. Bjorhovde, "Developments and advanced applications of concrete-filled steel tubular (CFST) structures: Members," *Journal of Constructional Steel Research*, vol. 100, pp. 211–228, Sep. 2014, https://doi.org/10.1016/j.jcsr.2014.04.016.

[17] S. Motoo and M. Kazuaki, "Experimental Study on Ultimate Behavior of Ultra-High-Strength Concrete-Filled Steel Pipe Shear-Bending Columns," *Proceedings of the Department of Construction of the Architectural Institute of Japan*, vol. 64, no. 520, pp. 133–140, 1999, https://doi.org/10.3130/aijs.64.133_2.

[18] Q. Yu, Z. Tao, and Y.-X. Wu, "Experimental behaviour of high performance concrete-filled steel tubular columns," *Thin-Walled Structures*, vol. 46, no. 4, pp. 362–370, Apr. 2008, https://doi.org/10.1016/j.tws.2007.10.001.

[19] P. C. Nguyen, D. D. Pham, T. T. Tran, and T. Nghia-Nguyen, "Modified Numerical Modeling of Axially Loaded Concrete-Filled Steel Circular-Tube Columns," *Engineering, Technology & Applied Science Research*, vol. 11, no. 3, pp. 7094–7099, Jun. 2021, https://doi.org/10.48084/etasr.4157.

[20] A. N. Hassooni and S. R. A. Zaidee, "Behavior and Strength of Composite Columns under the Impact of Uniaxial Compression Loading," *Engineering, Technology & Applied Science Research*, vol. 12, no. 4, pp. 8843–8849, Aug. 2022, https://doi.org/10.48084/etasr.4753.

[21] Z. H. Abdulghafoor and H. A. Al-Baghdadi, "Static and Dynamic Behavior of Circularized Reinforced Concrete Columns Strengthened with Hybrid CFRP," *Engineering, Technology & Applied Science Research*, vol. 12, no. 5, pp. 9336–9341, Oct. 2022, https://doi.org/10.48084/etasr.5162.